Author(s): Kaukonen, M. & Nieminen, R. M.

Title: Atomic-scale modeling of the ion-beam-induced growth of amorphous carbon

Year: 2000

Version: Final published version

Please cite the original version:

Kaukonen, M. & Nieminen, R. M. 2000. Atomic-scale modeling of the ion-beam-induced growth of amorphous carbon. Physical Review B. Volume 61, Issue 4. 2806-2811. ISSN 1550-235X (electronic). DOI: 10.1103/physrevb.61.2806.

Atomic-scale modeling of the ion-beam-induced growth of amorphous carbon

M. Kaukonen and R. M. Nieminen
Laboratory of Physics, Helsinki University of Technology, P.O. Box 1100, FIN-02015 HUT, Finland
(Received 28 July 1999)

The results of a detailed molecular-dynamics study of the growth of amorphous carbon (a-C) are reported. Carbon atoms with kinetic energies between 10 and 150 eV are deposited on a-C surface originating from bulk a-C. Earlier simulation results of an optimal energy window at 40–70 eV are confirmed. Additionally, it is found that the growth rate is at maximum at around 40 eV. At low implantation energies ($E_{\mathrm{beam}} \approx 10$ eV), the growth of amorphous carbon takes place on the surface. At higher energies, the growth proceeds increasingly in the subsurface region by global film expansion and single atom diffusion towards the surface. Scattering events (e.g., the deposited atom does not adsorb to the surface) at intermediate energies $E_{\mathrm{beam}} \approx 100$ eV result in a densification of the growing film. Moreover, at $E_{\mathrm{beam}} \approx 150$ eV, nonpermanent diamond formation is observed.

I. INTRODUCTION

Technological interest in amorphous carbon (a-C) stems from the fact that it can be produced at usual laboratory conditions with reasonable growth rates (1 μm/h) and with properties close to that of crystalline diamond.[1] Currently there are an increasing number of commercial applications, such as hard surface coatings.[2] The possible electronics applications are the same as with diamond.[3] The main effort has focused on using a-C as a cathode material due its low electron affinity[4] or as a semiconductor material.[5,6] The latter interest is limited as well-controlled n-type doping of a-C has proven difficult.[7] A possible theoretical explanation for this failure is given by Sitch *et al.*[8] and by Stumm *et al.*[9]

The growth of a-C using neutral carbon atoms as the growth species has been modeled extensively. The early Heuristic work by Lifshitz *et al.* is based on experimental observations and physical intuition.[10] Lifshitz *et al.* propose a subplantation model where the colliding atom penetrates into the surface and causes local stress. When this stress is released, diamondlike bonds are formed in the subsurface region. An alternative growth model has been proposed by Marks *et al.*[11] They suggest that the collision induced stress is stochastically localized on the surface and not in the subsurface region, arguing that the growth proceeds directly on the surface and not in the bulk region. A recent molecular dynamics (MD) study by Uhlmann *et al.* with a density-functional tight-binding description of the interatomic forces, supports the subplantation model.[12] Our earlier study suggests that a low temperature of the substrate material favors the diamondlike properties.[13]

Koponen *et al.* suggest different time scales for different kinds of ordering processes in the growing film.[14] They divide the time after the impact into three stages. Their ''peening'' state is characterized by high pressure and temperature, lasting some tens of fs. Subsequent relaxation occurs until the local temperature has dropped below 2000 K. Thereafter long-time scale relaxation and diffusion events may take place.

A great deal of experimental work has been carried out in this field.[15,16] Most recently, Davis *et al.* use 35–320 eV carbon ions beams to study a-C surfaces experimentally.[17] They observe a sp^2-rich layer on the top of the surface up to the ion penetration depth where the film turns to sp^3 rich. They propose that the bonds convert from sp^2 to sp^3 at the sp^2-sp^3 interface causing simultaneously the film to expand.

The objective of this study is threefold. First, the aim is to analyze the final a-C structures grown at various simulated ion-beam deposition energies. Secondly, we strive to clarify the atomic processes in a single deposition event, e.g., how deep do the deposited atoms penetrate in the film and what is the duration of the ''thermal spike'' after a deposition event. Thirdly, and perhaps most importantly, the purpose is to study the growth process itself. Where do the new bonds form and are there diamondlike or graphitelike domains in the growing a-C film? What is the role of the beam energy in these questions?

The paper is organized as follows. The simulation method and the preparation of the substrate are described in Sec. II. Simulation results are presented in Sec. III, and conclusions follow in Sec. IV.

II. SIMULATION METHOD AND THE MODEL SYSTEM

The simulations in this work are done using classical molecular dynamics with the empirical Tersoff potential for the carbon-carbon interactions.[18] This potential has been successfully applied to amorphous carbon (a-C) (Ref. 19) as well as to other covalent systems such as Si.[20]

The a-C substrate is prepared as follows. A bulk sample of the experimentally observed density 3.0 g/cm^3 is made by randomly positioning 438 carbon atoms in a supercell with dimensions 14.28 Å$\times$14.28 Å$\times$14.28 Å. This bulk system is allowed to follow the Newtonian equations of motion for 10 ps. In order to minimize the total energy of the system, the sample is thereafter kept at 5000 K for 10 ps, and is finally cooled to 0 K in 10 ps, corresponding to a cooling rate of 5×10^{14} K/s. The periodic boundary condition is released in the surface normal [001] direction keeping the atoms in a 5 Å thick slice at the bottom of the surface fixed, to mimic an infinitely deep surface. The surface is allowed to evolve freely for 10 ps and then cooled to 0 K in 10 ps.

TABLE I. The sp ratios of the grown films. 200 topmost surface atoms are included in the analysis.

Energy	$nn>4$	sp^3	sp^{2+x}	sp^2	sp^{1+x}	sp^{ill} or $(nn=1)$ (%)
10 eV	0.0	28.5	14.0	46.5	11.0	0.0 (0.0)
40 eV	0.5	25.5	15.0	46.0	12.0	1.0 (0.0)
100 eV	0.0	24.0	9.0	51.5	14.5	1.0 (0.5)
150 eV	0.0	15.5	12.5	55.0	15.5	1.5 (0.5)

Again, the purpose is to reach a minimum in the total energy.

In order to mimic nonequilibrium growth conditions 300 carbon atoms with the beam energy 100 eV using a deposition interval of 10 ps are allowed to collide with the surface. Thereafter 200 carbon atoms are deposited onto the surface with various deposition energies. The data analysis presented in this paper is based on a further 100 atom deposition with each beam energy $E_{\text{beam}}=10,40,100$, and 150 eV. This kind of surface preparation was found to be necessary in order to study the growing film. This is because the properties of the atom-by-atom grown surface differ from the surfaces prepared by direct energy minimization techniques.

After a single deposition event the system is allowed to follow the unconstrained Newtonian equations of motion for 100 fs with a time step (dt) of 0.05 fs. Thereafter the system is cooled towards 0 K using a cooling algorithm introduced by Berendsen[21] with the cooling parameter $\tau_T=10$ fs. The temperature scaling is applied every 100th time step for 100–1000 fs after a deposition event using $dt=0.1$ fs. For the rest of the simulation after a deposition event (1–10 ps) $dt=0.2$ fs is used and the cooling is applied every 10th time step.

The time-dependent (e.g., instant) surface position in the surface normal direction is defined as the average height of ''surface'' atoms. These ''surface'' atoms are defined as having no other atoms in a cylinder of radius 1.6 Å and height 10 Å above them, the other atoms are labeled as bulk atoms. The ''surface'' atoms having less than two neighbors are excluded when defining this time dependent surface position. In the following sections, the deposition events are divided into three classes. First, an event is labeled as ''scattering,'' if the deposited atom does not bind to the surface in 100 fs. Secondly, ''surface-deposition'' takes place when $z>-2$ Å ($z=0$ defining the instant surface position). Thirdly, events with $z<-2$ Å are classified as subplantation events.

III. RESULTS

A. Final structures

The structural properties of slices consisting of 200 topmost atoms of the grown surfaces are presented in Tables I and II. The highest density and the largest atomic coordination numbers are obtained with $E_{\text{beam}}=40,100$ eV, as expected from the earlier studies.[11,19] The sp^3 ratio decreases with increasing E_{beam}, whereas the fraction of the twofold and threefold atoms increases with increasing E_{beam}. The fact that $E_{\text{beam}}=10$ eV leads to the largest average coordination number and sp^3 ratio, but not to the highest density, suggests that films grown with $E_{\text{beam}}=10$ eV are more porous than the films with $E_{\text{beam}}=40$ or 100 eV. The ring statistics shows interestingly that small carbon rings are present only with $E_{\text{beam}}=10$ or 40 eV. There is one four-ring with $E_{\text{beam}}=10$ eV and two four-rings on the surface with $E_{\text{beam}}=40$ eV in the 200-atom samples. Deeper in the film there is one three-ring with $E_{\text{beam}}=10$ eV. At the highest energy 150 eV, less rings are formed indicating a preferred formation of atom chains instead of rings. The net growth has a clear maximum at $E_{\text{beam}}=40$ eV (Table III), because the probability of a deposited atom to adsorb on the surface increases only slowly with increasing energy, but the probability of desorption of the surface atoms (e.g., sputtering) increases rapidly above 40 eV.

TABLE II. Structural properties of the grown films. The data is calculated from a 10 Å thick slice at the top of the surface. nn_{ave} is the average coordination number and ρ the density.

Energy	ρ g/cm^3	nn_{ave}
10 eV	2.85	3.18
40 eV	3.03	3.15
100 eV	3.03	3.08
150 eV	2.74	2.97

TABLE III. The number of subplanted atoms, the number of the surface-deposited atoms and the number of the scattered atoms. The total number of deposited atoms is 100. An atom is classified as subplanted if $z<-2$ Å and as surface deposited with $z>-2$ Å. Scattered atoms are the deposited atoms that are not bonded to the surface in 100 fs after the collision. The net growth is the increase in the number of atoms in the film, e.g., the atoms that adsorb on the surface minus the sputtered atoms.

Energy	Subplantation	On surface	Scattered	Net growth
10 eV	0	69	31	59
40 eV	1	87	12	75
100 eV	42	46	12	50
150 eV	61	32	7	43

B. Single deposition events

The average kinetic energy barriers (E_{barr}) for different beam energies are listed in Table IV. E_{barr}, following Uhlmann *et al.*[22] is defined as the kinetic energy loss of the deposited atom from the initial vacuum state to the first potential energy minimum of the system. It thus measures, how much kinetic energy of the deposited atom transforms to the increase in the potential energy of the system at the beginning of the collision phase. As can be seen from Table IV, an

TABLE IV. The kinetic energy barriers and the duration of the thermal spike ($T>3000$ K). The three different time estimates in the third column correspond to subplantation, surface deposition and scattering, respectively. The standard deviations are given in brackets.

Energy	E_{barr} (eV) [std]	$t(T>3000$ K)
10 eV	7.64 [2.2]	−,20 fs, 60 fs
40 eV	35.2 [5.3]	−,20 fs, 70 fs
100 eV	79.4 [22]	20 fs, 30 fs, 200 fs
150 eV	119 [35]	30 fs, 80 fs, 300 fs

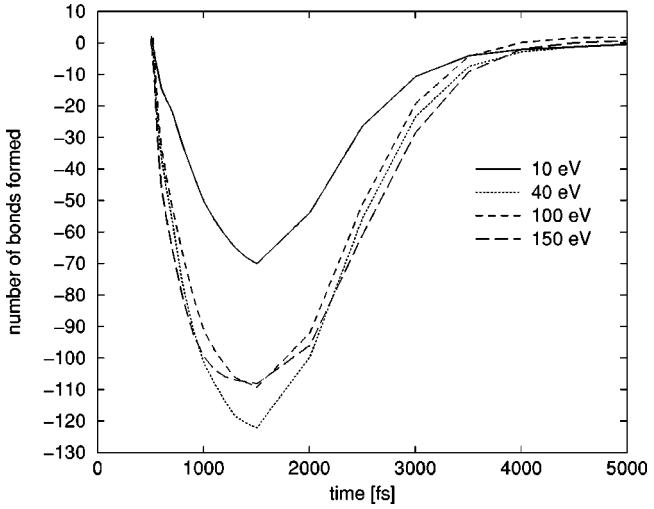

FIG. 1. The average bond destruction and annealing after a deposition event when the final position of the deposited atom is on the surface ($z > -2$ Å, i.e., surface deposition). The deposition takes place at $t = 500$ fs.

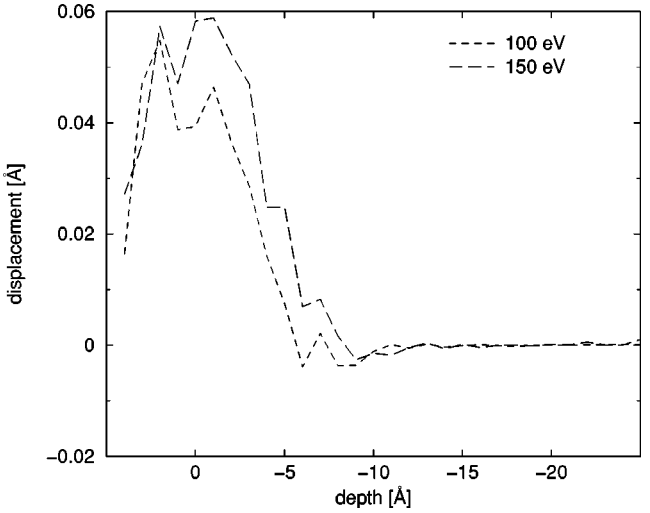

FIG. 2. The average displacements of the atoms in the growing film after a deposition event, when subplantation takes place ($z < -2$ Å). The instant surface position is at 0 Å.

increasing ratio of the energy remains as the kinetic energy of the deposited atom when increasing E_{beam}. This is because the surface atoms have less time to respond (e.g., increase their potential energy) to the impinging atom at the higher energies. E_{barr} depends also strongly on the lateral position of the impinging atom, as can be inferred from the standard deviations in Table IV.

The duration of the ''thermal spike'' (e.g., $T > 3000$ K) after a single collision is given in Table IV. The duration is always less than 300 fs in this energy range (10–150 eV). Scattering makes the $T > 3000$ K period longer. The motivation of the choice of 3000 K is the same as in Ref. 23: most atomic rearrangements take place above 3000 K. Our result supports the conclusion of Marks[23] that the duration of the thermal spike is of the order of 100 fs in *a*-C. However, bonds are broken and formed up to 5 ps (Fig. 1).

The penetration depths with respect to the instant surface position are given in Table V. The penetration depths have been studied earlier on diamond (111) surfaces by Uhlmann *et al.*[24] As expected, the penetration depth increases with the beam energy. At 100 eV the deposited atom recoils backwards to the surface direction after a maximal average depth of -3.6 Å. In the 150 eV case, however, the deposited atom does not return towards to the surface but remains at the maximal penetration depth. This indicates that the substrate is seriously damaged below the incorporated atom. Our estimates for the penetration depths are lower than those proposed by Davis *et al.*[17] However, the depth at which the surface expansion begins agrees rather well with their penetration depth (Fig. 2). The final potential energy of the deposited atom is on the average $-4.4, -5.0, -6.1$, and -6.0 eV with $E_{\mathrm{beam}} = 10, 40, 100$, and 150 eV, respectively. The deposited atom has the lowest potential energy at the end of the deposition interval (10 ps), except with $E_{\mathrm{beam}} = 40$ eV. In this case the the minimum energy is obtained approximately 1 ps after the deposition. This may indicate that relaxations in the film are less local in the 40 eV case compared to the other beam energies.

TABLE V. The final and maximum penetration depths [Å] and the corresponding coordination numbers. The time required to obtain the maximum depth and the maximum number of neighbors is given in parenthesis. Scattering events are excluded. The standard deviations are given in brackets.

Energy	z_{fin} [std], nn_{fin}	z_{max}, nn_{max}
10 eV	1.98 [1.6], 2.09	1.48 (30 fs), 2.85 (1000 fs)
40 eV	0.75 [1.4], 2.45	0.54 (40 fs), 2.85 (1000 fs)
100 eV	-1.94 [1.2], 3.09	-3.63 (50 fs), 3.59 (20 fs)
150 eV	-3.62 [1.8], 3.16	-3.63 (50 fs), 3.84 (20 fs)

C. Growth

The average number of bonds formed after a single deposition event is depicted in Fig. 1, in the case when the final position of the deposited atom is on the surface ($z > -2.0$ Å, i.e., surface deposition). In the subplantation case ($z < -2.0$ Å) the damage is of the order of 10% more severe. When the deposited atom scatters, the damage is slightly smaller. Scattering event is defined here so that the deposited atom is not bonded to the surface in 100 fs after the collision. The bond destruction is most serious for roughly 1 ps after the impact. Approximately 60 to 120 bonds are destroyed at $t = 1$ ps, the damage increasing with the increasing deposition energy. These numbers are lower limits to the true bond destruction, because of the finite size of the supercell. As can be seen in Fig. 1, the annealing requires approximately 5 ps. Generally, the main reason for the depletion of bonds is the decrease of the number of fourfold coordinated atoms in the subsurface region, as can be seen in Fig. 3. At the same time the number of threefold coordinated atoms increases considerably (Fig. 4). With $E_{\mathrm{beam}} = 150$ eV the increase in the number of threefold and the decrease in the number of fourfold coordinated atoms take place in a shorter time scale, about 500 fs compared to 3–5 ps in all other cases. This very special case occurs only when the final position of the deposited atom is on the surface ($z > -2.0$ Å). There is a increase in the number of

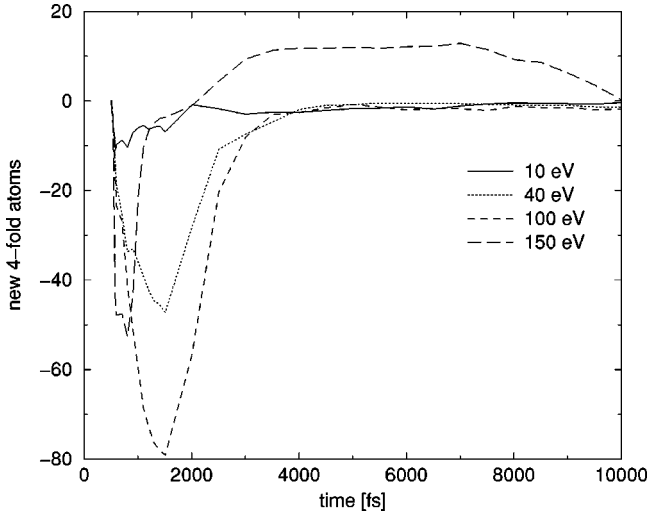

FIG. 3. The average formation of fourfold coordinated atoms in the subsurface region. The deposition takes place at $t=500$ fs. The final position of the deposited atom is on the surface ($z>-2$ Å, i.e., surface deposition).

fourfold atoms and decrease in the number of the threefold atoms for 3–7 ps after the deposition event. However, this diamond-formation phenomenon disappears when the annealing period exceeds 8 ps (Figs. 3, 4). Our explanation for this transient phenomenon is that the deposited atom collides with more than one of the surface atoms transferring its kinetic energy to these surface atoms. These surface atoms penetrate simultaneously deeper into the growing film making it more diamondlike.

The numbers of new bonds formed in one deposition event are summarized in Table VI. The cumulative number of new bonds is depicted in Fig. 5 in the case when the deposited atom remains near the surface ($z>-2.0$ Å). At low energies (10 and 40 eV) on the average 2.5 and 2.1 bonds are formed when the final position of the deposited atom is on the surface (which is the case for 70 and 90% of these deposition events, respectively). At 10 eV the new bonds are formed on the surface: the deposited atom adsorbs on the top of the growing surface making the atom(s) below it ''bulklike'' according our definition (see the preceding section). At 40 eV the deposited atom penetrates just below the topmost atoms of the film, so that no new surface bonds are formed. At higher energies atoms from subsurface layers diffuse to the top of the film and new surface bonds may form. When scattering occurs, bond breaking takes place (-0.5 and -1.1 bonds/event) at these energies. At 100 eV, when the deposited atom remains on the surface, the bond formation is again of order 2.5 bonds/event decreasing to 1.2 bonds/event at 150 eV. Subplantation ($z<-2$ Å) results in fewer bonds, especially at 100 eV only 1.3 bonds/event are formed. In this case there is a simultaneous bond formation-bond breaking process. The surface bonds are destroyed but the destruction is compensated by new bulk bonds just below the surface. The surface bond destruction may stem from the abstraction of the surface atoms with no compensating rearrangements on the surface. At 150 eV and subplantation there is a small increase in the number of surface bonds, which is due to the diffusion of atoms locating initially deeper in the film. The total number of bonds is increasing at 100 eV with subplantation up to of order 10 Å deepness. At 150 eV there is decrease in bond formation in 5–10 Å depth, reflecting the increasing dam-

TABLE VI. The average number of bonds formed in one deposition event. In the summation, the bulk bonds and surface bonds (respectively) are added yielding the total number of new bonds.

Energy	Subplantation	On surface	Scattered
10 eV		$1.5+1.0=2.5$	$-0.2-0.3=-0.5$
40 eV		$2.0+0.1=2.1$	$-2.2+1.1=-1.1$
100 eV	$2.4-1.1=1.3$	$1.4+1.2=2.6$	$2.8-0.1=2.7$
150 eV	$1.4+0.5=1.9$	$3.9-2.2=1.7$	$0.2-0.1=0.1$

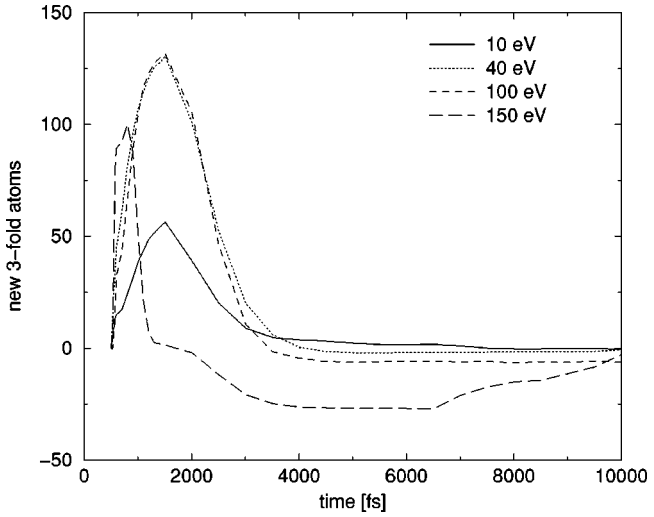

FIG. 4. The average formation of threefold coordinated atoms in the subsurface region. The deposition takes place at $t=500$ fs. The final position of the deposited atom is on the surface ($z>-2$ Å, i.e., surface deposition).

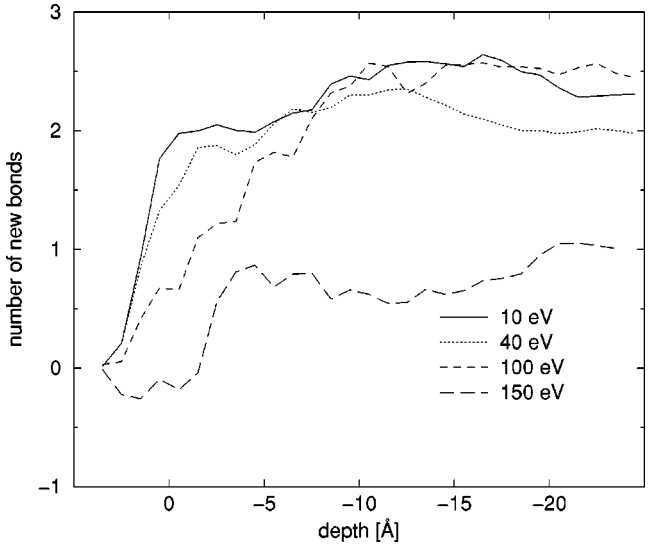

FIG. 5. The average cumulative number of neighbors in one event, when the deposited atom is on the surface region ($z>-2$ Å, i.e., surface deposition). The instant surface position is at 0 Å.

TABLE VII. Number of atoms making transition from surface to bulk. The scattering events are excluded. The deposited atom is considered initially as a surface atom.

Energy	surface → bulk
10 eV	1.1
40 eV	2.5
100 eV	6.9
150 eV	7.6

age caused by the collision cascade. Below this damaged area a new densification is taking place at the depth of the order of 15 Å, resembling the growth model suggested by Uhlmann.[12] The overall bond formation at 150 eV is lower compared to the other beam energies. Interestingly, at $E_{\mathrm{beam}}=100$ eV, the scattering of the deposited atom leads to film densification (Table VI). This is due to the surface atoms penetrating to the subsurface region, making the film denser.

In Table VII the number of atoms changing their status from surface to bulk atoms is shown. These data clearly support the subplantation model at $E_{\mathrm{beam}}\geqslant 40$ eV because surface atoms penetrate into the surface and become bulklike. (For the definition of a surface atom, see the end of Sec. II.) Even with 10 eV the deposited atom may replace a near-surface ''bulk'' atom and the former bulk atom becomes a surface atom. This process is illustrated in Fig. 6(a). On the other hand, with higher energies this indicates that the film not only expands as a whole but also individual atoms diffuse to the surface from the subsurface region. The global film expansion is shown in Fig. 2. The overall picture of the film growth is schematically given in Fig. 6.

D. Diamond and graphite formation

The transition to a diamondlike configuration requires a higher local temperature and a bigger pressure fluctuation when compared to the transition to graphite (we use a local pressure definition given by Laakkonen and Nieminen[25]). The transition to diamondlike atom from a threefold coordinated atom requires at least 500–1700 K whereas a transition to graphite occurs at 100–500 K lower temperatures, depending on the beam energy. The pressure pulse required for a diamond transition is on the average double in magnitude compared to a graphitic transition. The average maximum in the pressure pulse (corresponding to stretching of bonds) for atoms making the transition from threefold coordination to diamond are $+20$ GPa at energies 40–150 eV and $+4$ GPa at $E_{\mathrm{beam}}=10$ eV. The values for the minimum of the pressure pulse (corresponding to compression of bonds) are -20 GPa at energies 40–150 eV and -5 GPa at $E_{\mathrm{beam}}=10$ eV.

This fact is also reflected in the transition depths. The transition to diamond occurs near the surface (at average depths of $+0.5,-0.6,-2.5$, and -3.6 Å). The graphitic transition takes place deeper in the growing film at the depth of $-2--10$ Å. Only at 150 eV the average transition depths mix because of the serious damage caused by the collision cascade. Otherwise the diamond transition region is located closer to the surface than region for the transition to graphite.

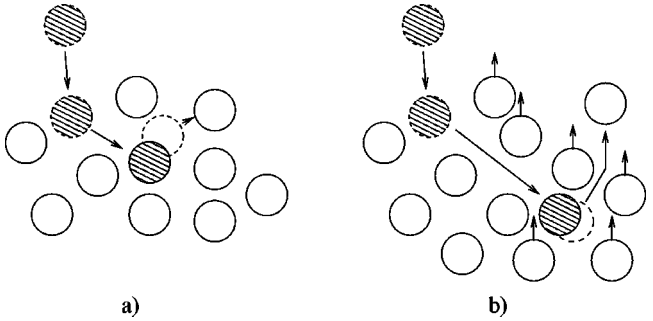

FIG. 6. (a) At low energies the deposited atom may replace a former bulk atom. (b) With higher energies subplantation may occur. The film grows by global expansion and individual atom diffusion. The deposited atom is a filled ball. The intermediate positions are dashed.

IV. CONCLUSION

To conclude, the growth of amorphous carbon proceeds on the surface at low beam energies ($E_{\mathrm{beam}}\approx 10$ eV). At higher energies, the growth is increasingly taking place in the subsurface region by global film expansion and single atom diffusion towards the surface. Our results support in general the subplantation model,[10] while the surface growth model by Marks *et al.*[11] remains valid at low energies ($E_{\mathrm{beam}}\approx 10$ eV). The transition to diamond occurs mostly near the surface (a few Å below the instant surface position). This transition region moves deeper in the film with increasing beam energy. Scattering events (see Sec. II for definitions) at $E_{\mathrm{beam}}\approx 100$ eV force the surface atoms to impinge into the film increasing the film density. This suggests that codeposition with inert heavy ions with suitable kinetic energy might enhance the film quality. The growth rate is found to depend strongly on the implantation energy. It has a maximum at around 40 eV implantation energy. Interestingly, at $E_{\mathrm{beam}}\approx 150$ eV and when the deposited atom remains on the top of the surface (e.g., surface deposition), there is a time window (3–7 ps after the deposition) when the diamond formation is enhanced in the subsurface region. This suggests that varying the cooling rate might make the diamond nucleation more permanent.

ACKNOWLEDGMENTS

This research has been supported in part by the Academy of Finland. We acknowledge the generous computer resources provided by the Center of Scientific Computing. We thank Dr. P. Sitch for a critical reading of the manuscript, and Dr. J. Koskinen and Dr. S. Uhlmann for stimulating discussions.

[1] J. Robertson, Adv. Phys. **35**, 317 (1986).
[2] T.C.S. Vandevelde, K. Vandierendonck, M. Van Stappen, W. Du Mong, and P. Perremans, Surf. Coat. Technol. **113**, 80 (1999).
[3] J. F. Prins, in *The Physics of Diamond*: *Proceedings of the International School of Physics ''Enrico Fermi,''* Course CXXXV (IOS Press, Amsterdam, 1997), pp. 411–484.
[4] B.S. Satyanarayana, A. Hart, W.I. Milne, and J. Robertson, Appl. Phys. Lett. **71**, 1430 (1997).
[5] K. Okano, H. Kiyota, T. IIwasaki, T. Kurosu, M. Iida, and T. Nakamura, Appl. Phys. Lett. **58**, 840 (1991).
[6] J.W. Glesener, A.A. Morrish, and K.A. Snail, J. Appl. Phys. **70**, 5144 (1991).
[7] V.S. Veerasamy, J. Yuan, G.A.J. Amaraunga, W.I. Milne, K.W.R. Gilkes, M. Weiler, and L.M. Brown, Phys. Rev. B **48**, 17 954 (1993).
[8] P.K. Sitch, Th. Köhler, G. Jungnickel, D. Porezag, and Th. Frauenheim, Solid State Commun. **100**, 549 (1996).
[9] P. Stumm, D.A. Drabold, and P.A. Fedders, J. Appl. Phys. **81**, 1289 (1997).
[10] Y. Lifshitz, S.R. Kasi, and J.W. Rabalais, Phys. Rev. Lett. **62**, 1290 (1989).
[11] N.A. Marks, D.R. McKenzie, and B.A. Pailthorpe, Phys. Rev. B **53**, 4117 (1996).
[12] S. Uhlmann, Th. Frauenheim, and Y. Lifshitz, Phys. Rev. Lett. **81**, 641 (1998).
[13] M. Kaukonen and R.M. Nieminen, Surf. Sci. **331-333**, 975 (1995).
[14] I. Koponen, M. Hakovirta, and R. Lappalainen, J. Appl. Phys. **78**, 1 (1995).
[15] J. Koskinen, Appl. Phys. Lett. **47**, 941 (1985).
[16] J. Kulik, G.D. Lempert, E. Grossman, D. Marton, J.W. Rabalais, and Y. Lifshitz, Phys. Rev. B **52**, 15 812 (1995).
[17] C.A. Davis, G.A.J. Amaratunga, and K.M. Knowles, Phys. Rev. Lett. **80**, 3280 (1998).
[18] J. Tersoff, Phys. Rev. Lett. **61**, 2879 (1988).
[19] H.-P. Kaukonen and R.M. Nieminen, Phys. Rev. Lett. **68**, 620 (1992).
[20] J. Tersoff, Phys. Rev. B **37**, 6991 (1988).
[21] H.J.C. Berendsen, J.P.M. Postma, W.F. van Gunsterer, A. DiNola, and H.R. Haak, J. Chem. Phys. **81**, 3684 (1984).
[22] S. Uhlmann, Th. Frauenheim, K.J. Boyd, D. Marton, and J.W. Rabalais, Radiat. Eff. Defects Solids **141**, 185 (1997).
[23] N.A. Marks, Phys. Rev. B **56**, 2441 (1997).
[24] S. Uhlmann, Th. Frauenheim, and U. Stephan, Phys. Rev. B **53**, 4117 (1996).
[25] J. Laakkonen and R.M. Nieminen, Phys. Rev. B **41**, 3978 (1990).